

Phenomenological theory of the anomalous normal-state transport properties of iron pnictides

P. Prelovšek^{1,2} and I. Sega¹¹*J. Stefan Institute, SI-1000 Ljubljana, Slovenia*²*Faculty of Mathematics and Physics, University of Ljubljana, SI-1000 Ljubljana, Slovenia*

(Received 16 December 2009; revised manuscript received 10 February 2010; published 16 March 2010)

We employ the phenomenological theory of the quasiparticle relaxation based on the simplified two-band description and the spin-fluctuation mediated interband coupling to analyze recent normal-state transport data in electron-doped iron pnictides, in particular the $\text{Ba}(\text{Fe}_{1-x}\text{Co}_x)_2\text{As}_2$ family. The temperature and doping dependence of the resistivity, thermopower, and the Hall constant are evaluated. We show that their anomalous behavior emerging from experiments can be consistently described within the same framework assuming also “marginal,” i.e., non-Fermi-liquid-like spin fluctuations provided, however, that the interband coupling is quite strong. We also show that a large thermopower as experimentally observed results from an asymmetric energy-dependent quasiparticle relaxation rate and due to the semimetallic character of both bands.

DOI: [10.1103/PhysRevB.81.115121](https://doi.org/10.1103/PhysRevB.81.115121)

PACS number(s): 71.27.+a, 75.20.-g, 74.72.-h

I. INTRODUCTION

The novel class of iron-based superconductors (SCs) (Refs. 1 and 2) reveals besides the high SC transition temperature T_c also several normal-state properties which are inconsistent with the usual Fermi-liquid (FL) description of metals. Regarding transport properties, magnetic ordering and spin fluctuations as well as the presumable unconventional SC iron pnictides (IPs) are quite close to SC cuprates. In the latter class at least part of the anomalous behavior emerges from the proximity to the Mott-Hubbard insulator³ and from strong correlations, i.e., strong electron-electron Coulomb repulsion. On the other hand, in IPs correlations seem to be less severe so the common point might be pronounced low-frequency spin fluctuations and a strong coupling of charge carriers to such collective modes.

The experimental evidence for the magnetic order and fluctuations comes most directly from elastic and inelastic neutron scattering (INS) showing the commensurate spin-density-wave (SDW), i.e., the antiferromagnetic (AFM) long-range order in the parent compounds.⁴ Recent INS results also confirm strong and anomalous AFM normal-state spin fluctuations⁵ as well as the resonant magnetic mode^{6,7} analogous to the well known phenomenon in SC cuprates. That spin fluctuations do not obey normal FL behavior follows also from NMR-relaxation results.^{8,9}

The IPs show generally large normal-state dc electrical resistivity $\rho(T)$. Its systematics has been first studied in the family emerging from the parent (undoped) compound LnFeAsO (LFAO) with a variety of lanthanides $\text{Ln}=\text{Ce-Dy}$ where the electron doping has been achieved either by doping with F, e.g., in $\text{LnFeAsO}_{1-x}\text{F}_x$ (LFAO)^{10–12} or via the oxygen deficiency LnFeAsO_{1-y} .¹³ Generally $\rho(T)$ is very high comparable to underdoped cuprates.¹⁴ The behavior changes from a SDW semimetal $x, y < 0.05$ over to the intermediate regime $x, y \sim 0.1$ with a nearly linear law $\rho \propto T$, into the overdoped regime with more FL-like $\rho \propto T^2$ behavior for $y > 0.2$. It is not yet evident to what extent very large $\rho(T)$ are due to polycrystalline character or measured samples since only recently single-crystal data become available.¹⁵ On the other hand, similar behavior appears in recently stud-

ied single-crystal class of electron-doped (so-called 122) family $\text{AE}(\text{Fe}_{1-x}\text{TM}_x)_2\text{As}_2$ where various alkali elements $\text{AE}=\text{Ba, Sr, and Ca}$ and transition metals ($\text{TM}=\text{Co, Cu}$) are at present explored. In the following we will mostly concentrate on the $\text{Ba}(\text{Fe}_{1-x}\text{Co}_x)_2\text{As}_2$ (BaFeCoAs) compound most investigated so far where x represents an effective electron doping. In this system the qualitative behavior of $\rho(T)$ is similar to LFAO results although the values are substantially smaller.^{16,17} At the same time, the thermopower $S(T)$ is far from FL behavior $S \propto T$, both in the LFAO (Refs. 10 and 11) and in BaFeCoAs.¹⁸ The values become comparable to non-degenerate electrons, i.e., $|S| \sim s_0 = k_B/e_0 = 86 \mu\text{V/K}$ with the maximum typically at $T \sim 100$ K, again resembling underdoped cuprates.¹⁹ A similar message is emerging from strongly T -dependent Hall constant $R_H(T)$ in LFAO (Ref. 20) and in BaFeCoAs.^{16,17}

Our aim is to extend the phenomenological analysis based on the simplified two-band model coupled via spin fluctuations as introduced previously²¹ and apply it for a semiquantitative description of the transport properties of the electron-doped IPs, here focusing on the BaFeCoAs compound. Starting with the evaluation of the anomalous T dependence of the quasiparticle (QP) damping rates, in particular in the electron band $\Gamma^e(\omega)$, we analyze within the same framework the dc transport quantities $\rho(T)$, $S(T)$, and $R_H(T)$. To explain anomalous $\rho(T)$ it is essential to assume quite strong coupling to non-FL-type spin fluctuations. On the other hand, large $S(T)$ can emerge only via a very asymmetric $\Gamma^e(\omega)$ and due to the semimetal character (low effective Fermi energies) of both bands. The previous approach²¹ is here upgraded with an explicit evaluation of T -dependent $\Gamma^e(\omega)$ and corresponding dc transport quantities without further simplifications. Qualitatively one can follow the development from a non-FL behavior to a more normal FL-type regime by changing the carrier concentration and the character of the input spin fluctuations by introducing a crossover temperature T^* controlling the extent of non-FL vs normal FL behavior thus simulating the experimental findings in BaFeCoAs as well as in the LFAO system.

In Sec. II we describe the phenomenological model as introduced previously²¹ and give some justification based on a more complete microscopic model. Section III presents the

lowest-order approximation for the QP damping $\Gamma(\omega)$ being the central ingredient for the understanding of the transport properties where its temperature and energy dependence are essentially controlled by the (phenomenological) ansatz for the spin-fluctuations mediated interband coupling as noted above. In Sec. IV basic equations for the dc transport quantities are presented. Results in different regimes of relevant parameters follow in Sec. V with a discussion of the approach and results in Sec. VI.

II. TWO-BAND MODEL

For the present analysis we adopt a simplified 2D model for IPs (Ref. 21) taking into account only two bands, an electron (e) band and a hole (h) band, both crossing the Fermi surface^{22–24} and coupled via spin fluctuations.²¹ In the folded Brillouin zone^{22,25} the h-like and e-like pockets are at $\mathbf{k} \sim 0$ and $\mathbf{k} \sim \mathbf{Q} = (\pi, \pi)$, respectively,

$$H_{ef} = - \sum_{\mathbf{k}, s} (\zeta_{\mathbf{k}}^e c_{\mathbf{k}s}^\dagger c_{\mathbf{k}s} + \zeta_{\mathbf{k}}^h d_{\mathbf{k}s}^\dagger d_{\mathbf{k}s}) + \frac{1}{\sqrt{N}} \sum_{\mathbf{k}, \mathbf{q}, ss'} m_{\mathbf{k}\mathbf{q}} \mathbf{S}_{\mathbf{q}} \cdot \sigma_{ss'} c_{\mathbf{k}-\mathbf{q}, s}^\dagger d_{\mathbf{k}s'} + \text{H.c.}, \quad (1)$$

and $c_{\mathbf{k}}, d_{\mathbf{k}}, (\zeta^e, \zeta^h)$ refer to electrons in e-like and h-like bands, respectively.

The following justification can be given for the above phenomenological model. The realistic electronic model for 2D IPs includes several (e.g., five) bands emerging from d orbitals of Fe. The interaction term is very complicated in general. Still the low-energy description (in the case of weak or modest electron-electron interactions) should contain only both bands at the Fermi surface (FS). So one of the relevant interaction terms generating the interband coupling in Eq. (1) can be written as²⁶

$$\tilde{H} = \sum \tilde{U} c_{\mathbf{k}s}^\dagger d_{\mathbf{k}'s'}^\dagger d_{\mathbf{k}''s''} c_{\mathbf{k}'''s''}. \quad (2)$$

The origin of the above interaction resides within a more complete multiorbital model, the interorbital and intraorbital Hubbard interactions U and V , respectively, as well as in the Hund's coupling J_H . The effective interaction, Eq. (2), could be rewritten as the coupling to a fluctuating SDW field

$$\mathcal{S}_{\mathbf{q}} = \tilde{U} \sum_{\mathbf{k}, ss'} \sigma_{ss'} c_{\mathbf{k}s}^\dagger d_{\mathbf{k}+\mathbf{q}s'}. \quad (3)$$

The SDW fluctuation $\mathcal{S}_{\mathbf{q}}$ should have in general, e.g., for the relevant $\mathbf{q} \sim \mathbf{Q}$ a finite projection on the usual spin operator $\mathbf{S}_{\mathbf{q}}$ (emerging from local moments), but this remains to be shown by an explicit consideration within the full multiorbital model for IPs.

III. QUASIPARTICLE DAMPING

In the evaluation of the transport properties we follow the approach introduced previously.²¹ We first consider the corresponding Green's functions for $\sigma = e, h$ [$\bar{\sigma} = (h, e)$] electrons $G_{\mathbf{k}}^\sigma(\omega) = [\omega^+ - \epsilon_{\mathbf{k}}^\sigma - \Sigma_{\mathbf{k}}^\sigma(\omega)]^{-1}$, where $\epsilon_{\mathbf{k}}^\sigma = \zeta_{\mathbf{k}}^\sigma - \mu$. The self-energies $\Sigma_{\mathbf{k}}^\sigma(\omega)$ are evaluated within the lowest-order

perturbation in the interband coupling, Eq. (1), induced by spin fluctuations entering via dynamical spin susceptibility $\chi_{\mathbf{q}}(\omega)$,

$$\Sigma_{\mathbf{k}}^\sigma(\omega) = 3 \sum_{\mathbf{q}} m_{\mathbf{k}\mathbf{q}}^2 \int \int \frac{d\omega_1 d\omega_2}{\pi} g_{12} \frac{A_{\mathbf{k}-\mathbf{q}}^{\bar{\sigma}}(\omega_1) \chi_{\mathbf{q}}''(\omega_2)}{\omega - \omega_1 - \omega_2},$$

$$g_{12} \equiv g(\omega_1, \omega_2) = \frac{1}{2} \left[\text{th} \frac{\beta\omega_1}{2} + \text{cth} \frac{\beta\omega_2}{2} \right]. \quad (4)$$

To proceed we make several simplifications, which are expected to apply to IPs in the low-doping regime close to the AFM (in the folded zone) instability, i.e., in the system without long-range AFM order. The spin fluctuations $\chi_{\mathbf{q}}''(\omega)$ in the normal phase are assumed to be centered at $\mathbf{q} \sim \mathbf{Q} = (\pi, \pi)$ and broad enough in the \mathbf{q} space relative to h/e pockets. This is indeed well visible in recent INS results for the BaFeCoAs system.⁵ Hence, we replace $\chi_{\mathbf{q}}(\omega) \sim \chi_{\mathbf{Q}}(\omega) = \tilde{\chi}(\omega)$. Since the relevant e/h bands form only small pocketlike FS we neglect in the low ω regime also the \mathbf{k} dependences of the self-energies; i.e., we replace $\Sigma_{\mathbf{k}}^\sigma(\omega) \sim \Sigma^\sigma(\omega)$ whereby $\mathbf{k} \sim 0$ and $\mathbf{k} \sim \mathbf{Q}$ are relevant for the h and e bands, respectively. Hence, with the local character of the self-energies the spectral function $A_{\mathbf{k}}^\sigma(\omega) = A^\sigma(\epsilon_{\mathbf{k}}, \omega)$ can be expressed as

$$A^\sigma(\epsilon_{\mathbf{k}}, \omega) = - \frac{1}{\pi} \text{Im} [\Omega^\sigma(\omega) - \epsilon_{\mathbf{k}}^\sigma + i\Gamma^\sigma(\omega)]^{-1}, \quad (5)$$

with $\Omega^\sigma(\omega) = \omega - \text{Re} \Sigma^\sigma(\omega) = \omega / Z^\sigma(\omega)$ and $\Gamma^\sigma(\omega) = -\text{Im} \Sigma^\sigma(\omega)$. Note that $Z^\sigma(\omega)$ and $\Gamma^\sigma(\omega)$ play the role of the QP weight and the QP damping, respectively.

The above approximations simplify the expression for the QP damping as it follows from Eq. (4),²¹

$$\Gamma^\sigma(\omega) = \frac{3}{2} \bar{m}^2 \int d\omega' g(\omega - \omega', \omega') \mathcal{N}^{\bar{\sigma}}(\omega - \omega') \tilde{\chi}''(\omega'), \quad (6)$$

where the effective interband coupling is $\bar{m} \sim m_{\mathbf{Q}, \mathbf{Q}} = m_{0, \mathbf{Q}}$ and $\mathcal{N}^{\bar{\sigma}}(\omega) = (2/N) \Sigma A_{\mathbf{k}}^{\bar{\sigma}}(\omega)$ are the e/h band single-particle densities of states (DOS).

Within the present analysis spin fluctuations are taken as a phenomenological input. In analogy with the anomalous QP and transport properties of cuprates³ we assume that the origin is in the non-FL character of $\chi_{\mathbf{q}}''(\omega)$ and a strong coupling of carriers to the latter. Indeed, recent INS results in electron-doped BaFeCoAs indicate a behavior very close to the one for marginal FL.⁵ For generality we therefore assume further on the form

$$\tilde{\chi}''(\omega) = \pi C(\omega) \text{th} \frac{\omega}{2(T + T^*)}, \quad (7)$$

where $C(\omega)$ is (for $T^* = 0$) the (symmetrized) dynamical spin correlation function. While $T^* = 0$ yields the marginal FL (Ref. 27) dynamical fluctuations, we can simulate with $T^* > 0$ the transition to the normal FL regime for low $T < T^*$. For simplicity also a smooth cutoff on $C(\omega) = C_0$ is imposed for $\omega > \omega^*$.

IV. DC TRANSPORT QUANTITIES

dc electrical conductivity σ_0 and the thermopower S can be expressed via general transport coefficients. For the isotropic transport in 2D and assuming separate contributions of both bands, transport coefficients L_{1n}^σ can be expressed within the linear-response theory in terms of spectral functions²⁸ provided also that vertex corrections are neglected,

$$L_{1n}^\sigma = -\frac{2\pi}{N} \sum_{\mathbf{k}} (v_{\mathbf{k}}^{\alpha\sigma})^2 \int d\omega \omega^{n-1} \frac{df}{d\omega} A_{\mathbf{k}}^\sigma(\omega), \quad (8)$$

with the Fermi function $f=1/[\exp(\omega/T)+1]$ and $v_{\mathbf{k}}^{\alpha\sigma}$ σ -band velocities ($\alpha=x,y$). Due to the \mathbf{k} -independent $\Sigma^\sigma(\omega)$ and Eq. (5) the actual expressions have the same form as used within the dynamical-mean-field theory,²⁹

$$L_{1n}^\sigma = -\pi \int \int d\omega d\epsilon \phi^\sigma(\epsilon) \omega^{n-1} \frac{df}{d\omega} [A^\sigma(\epsilon, \omega)]^2, \quad (9)$$

$$\phi^\sigma(\epsilon) = \frac{2}{N} \sum_{\mathbf{k}} (v_{\mathbf{k}}^{\alpha\sigma})^2 \delta(\epsilon - \epsilon_{\mathbf{k}}).$$

With known L_{1n}^σ one can express the final dc conductivity

$$\sigma_0 = e_0^2 L_{11} = e_0^2 (L_{11}^e + L_{11}^h), \quad (10)$$

as well as the thermopower

$$S_0 = -s_0 \frac{L_{12}}{TL_{11}}, \quad (11)$$

where $L_{12} = L_{12}^e + L_{12}^h$ and $s_0 = k_B / e_0$.

Within the same framework and approximations an analogous expression for the Hall conductivity has also been derived^{30,31} and applied to nontrivial models^{32,33}

$$\sigma_{xy}^\sigma = -\sigma_0^H \int \int d\omega d\epsilon \phi_H^\sigma(\epsilon) \frac{df}{d\omega} [A^\sigma(\epsilon, \omega)]^3, \quad (12)$$

where $\sigma_0^H = 2\pi^2 e_0^3 B / 3$ and

$$\phi_H^\sigma = \frac{2}{N} \sum_{\mathbf{k}} \left(\frac{\partial \epsilon_{\mathbf{k}}^\sigma}{\partial k_x} \right)^2 \frac{\partial^2 \epsilon_{\mathbf{k}}^\sigma}{\partial k_y^2} \delta(\epsilon - \epsilon_{\mathbf{k}}^\sigma). \quad (13)$$

Again, within the two-band model $\sigma_{xy} = \sigma_{xy}^e + \sigma_{xy}^h$ and

$$R_H = \frac{\sigma_{xy}}{B\sigma_0^2}. \quad (14)$$

It should be, however, recognized that Eq. (12) obtained via the linearization of the linear response in an external magnetic field $B > 0$ is less explored [as compared with transport coefficients Eq. (8)] and only partly tested in situations with nontrivial $\Gamma^\sigma(\omega) \neq \Gamma_0^\sigma$, in particular in the presence of correlations.³⁴

Transport quantities depend only on the QP properties close to the Fermi surface. Hence, we assume in the following calculations the simplified form for the unperturbed e/h bands, i.e., with 2D parabolic dispersions,

$$\epsilon_{\mathbf{k}}^e = \epsilon_0^e + t_e k^2, \quad \epsilon_{\mathbf{k}}^h = \epsilon_0^h - t_h k^2, \quad (15)$$

with (unrenormalized) effective masses $m^\sigma = 1/(2t^\sigma)$ (with lattice constant $a_0=1$) and the unperturbed DOS $\mathcal{N}_0^\sigma = 1/(2\pi t^\sigma)$. Corresponding $\phi^\sigma, \phi_H^\sigma$ functions follow from Eqs. (9) and (13),

$$\phi^\sigma(\epsilon) = 2t^\sigma |\epsilon - \epsilon_0^\sigma| \mathcal{N}_0^\sigma, \quad \phi_H^\sigma(\epsilon) = \pm 2t^\sigma \phi^\sigma(\epsilon). \quad (16)$$

On the other hand, the final DOS entering Eq. (6) involves the effects of nontrivial $\Sigma^\sigma(\omega)$ and is evaluated as

$$\mathcal{N}^\sigma(\omega) = -\frac{2}{\pi W^\sigma} \text{Im} \int \frac{d\epsilon}{\Omega(\omega) - \epsilon + i\Gamma(\omega)}$$

$$= \frac{2}{\pi W^\sigma} \left[\arctg \frac{\Omega^\sigma - \epsilon_0^\sigma + W^\sigma}{\Gamma^\sigma} - \arctg \frac{\Omega^\sigma - \epsilon_0^\sigma}{\Gamma^\sigma} \right], \quad (17)$$

where $W^\sigma = 4\pi t^\sigma$ is the bandwidth within the parabolic approximation. In addition, we assume that the densities of electrons within the e/h bands, i.e., $n_e = x_e$ and $n_h = 1 - x_h$, x_h being the density of holes, are fixed separately, so that at each $T > 0$ the sum rule,

$$n^\sigma = \int d\omega f(\omega) \mathcal{N}^\sigma(\omega), \quad (18)$$

should be satisfied leading in principle to a nontrivial shift of $\epsilon_0^\sigma(T)$ in Eq. (15) (with respect to the chemical potential).

V. RESULTS

The above equations fully determine the evaluation procedure for $\Sigma^\sigma(\omega)$ at any T and consequently of transport quantities $\rho_0(T), S(T), R_H(T)$. The main input parameters are the e/h concentrations x_e, x_h and the corresponding t^σ . We note that coupling to spin fluctuations has a meaningful dimensionless coupling constant

$$g_0 = \bar{m}^2 C_0 \sqrt{\mathcal{N}_0^h \mathcal{N}_0^e}. \quad (19)$$

In addition, results depend also on the FL temperature T^* in Eq. (7) and on the cutoff ω^* , the latter mainly influencing low- ω behavior through the QP weight $Z(\omega)$.

In the following we consider the electron-doped case $x_e > x_h$, as relevant, e.g., for the electron-doped BaFeCoAs. Obviously, here the transport properties are dominated by the transport within the e-type band, although at high T also hole pockets contribute partially. On the other hand, we realize that in such a case the treatment of minority (h) carriers is oversimplified, since even at modest $g_0 < 1$ the hole QPs become heavily renormalized $Z^h(\omega) \ll 1$ influencing also $\mathcal{N}^h(\omega)$. The latter could be an artifact of the lowest-order approximation for the QP damping, Eq. (6). To avoid rather unphysical properties of hole QP, we introduce for the latter a simplification $\Gamma^h(\omega) = \Gamma_\phi^h$. Note that Γ^h influences results only indirectly, i.e., entering the dominant e-band damping $\Gamma^e(\omega)$ via $\mathcal{N}^h(\omega)$. At the same time, the hole contribution to dc transport quantities remains subleading provided that $\Gamma_0^h > \Gamma^e(\omega \sim 0)$, in particular at low T .

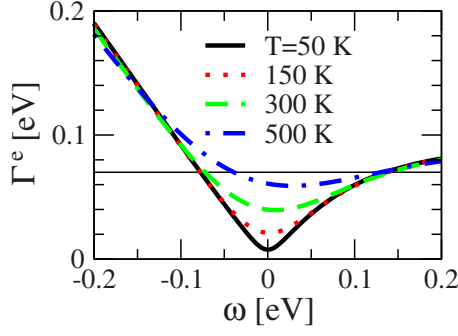


FIG. 1. (Color online) Electron-band QP damping $\Gamma^e(\omega)$ for various T for the intermediate doping. Horizontal line represents the chosen hole damping Γ_0^h .

Our aim is to show that the presented phenomenological theory can consistently as well as semiquantitatively account for the anomalous non-FL normal-state transport properties of (electron-doped) IPs, in particular for the large and T -linear $\rho(T)$, large thermopower $S(T)$ reaching quasiclassical values $|S| \sim s_0$, and T -dependent $R_H(T)$. Evidently, in the absence of a better understood microscopic model and relevant input parameters as the effective spin fluctuations, all varying between materials and different doping levels, we here mainly consider various possibilities and regimes which emerge from our analysis.

While displaying different regimes we fix some parameters. In the following we choose (unrenormalized) band parameters $t_e = 0.4$ eV and $t_h = 0.3$ eV and spin-fluctuation cut-off $\omega^* = 0.5$ eV. Actual levels of carrier concentrations x_e, x_h are not directly known in particular materials, since the doping x , e.g., with Co in BaFeTMAs, generally gives only partial information on $x = x_e - x_h$. To explain the anomalous properties it is, however, essential that x_h is low leading to a very asymmetric damping $\Gamma^e(\omega)$ and consequently to large values of $S(T)$. On the other hand, a disappearance of $x_h \rightarrow 0$ reduces strongly the scattering within the e band and the transport is expected to become more FL-like.

Evidently, the crucial parameter is the coupling strength g_0 . It most directly influences the resistivity $\rho(T)$ and in particular its derivative $d\rho(T)/dT$. To account quantitatively for $T \sim 300$ K experimental results for BaFeCoAs, we require modest $g_0 \sim \mathcal{O}(1)$ as discussed further on. On the other hand, much larger resistivities within the LFAO family indicate substantially larger $g_0 \gg 1$, as analyzed previously.²¹ It should be noted that due to constant Γ_0^h and x_h iterations of Eq. (4) are not needed but still μ should for each T separately be determined to keep x_e fixed.

Let us start with the case representing presumably the anomalous intermediate doping. For actual results presented in Figs. 1 and 2 we choose fixed concentrations $x_e = 0.2$, $x_h = 0.08$ while the remaining parameters are $g_0 = 1.6$, $T^* = 0$, and $\Gamma_0^h = 0.07$ eV. In Fig. 1 we first present the variation of $\Gamma^e(\omega)$ around $\omega \sim 0$ for various T . Since $T^* = 0$ the general behavior is of the MFL-type, i.e., roughly $\Gamma^e \propto \max(|\omega|, T)$.²¹ But as well important is a pronounced asymmetry with respect to $\omega = 0$ which emerges from low $x_h \ll 1$ and from the strong scattering on ω -dependent \mathcal{N}^h . The corresponding $\rho(T)/\rho_0$ and $S(T)/S_0$ are presented in Fig. 2. Note that within a 2D

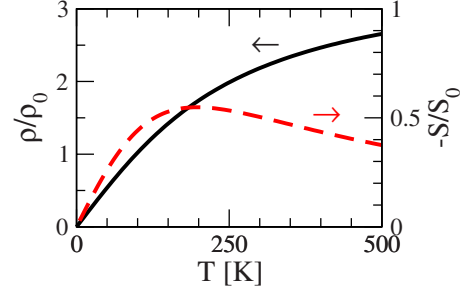


FIG. 2. (Color online) The resistivity $\rho(T)/\rho_0$ (full line; left scale) and the thermopower $S(T)/S_0$ (dashed line; right scale) for the intermediate electron-doped IPs.

layer $\rho_0 = \hbar/e_0^2 = 41.5$ k Ω . For actual BaFeCoAs materials with the interlayer distance $c_0 \sim 1.3$ nm this corresponds to $\tilde{\rho}_0 = c_0 \rho_0 \sim 0.5$ m Ω cm. As a consequence of the MFL-type $\Gamma^e(\omega)$ also $\rho(T)$ displays a linear variation for lower $T < 300$ K with a tendency to a saturation at higher T . Even more anomalous is $S(T)$ reaching a minimum at low $T \sim 150$ K with anomalously large (for a metal) value $S \sim -0.5s_0$. The decrease in $|S|$ at higher T results mainly from the compensation effect between e-band and h-band contributions.

The effect of a nonzero FL temperature T^* in Eq. (7) is presented in Fig. 3. At $T^* = 0$ the MFL-type variation is evident in the linear resistivity $\rho \propto T$ in Fig. 3(a). Finite $T^* > 0$ induces more normal FL-type variation $\rho \propto T^2$ for $T < T^*$. At the same time also the $S(T)$ changes gradually from an anomalously large and nonmonotonous variation at $T^* = 0$ into more normal FL-type $S \propto T$ for large $T^* = 1000$ K. The Hall constant $r_H(T) = R_H(T)/R_H^0$ (where $R_H^0 = V_0/e^2$, V_0 being the volume of the unit cell) is less sensitive on the non-FL behavior. Still it shows pronounced T variation for $T^* = 0$ emerging from a nontrivial electron/hole compensation and linear $\rho_e(T) \propto T$. Finally, at large T^* one sees in Fig. 3(c) rather constant $r_H(T) \propto 1/x_e$ as appropriate for a normal metal.

As last, we discuss the variation with the electron doping δn_e . We assume as the parent system the semimetal with finite $x_e^0 = x_h^0 = 0.15$. The effect of doping leads then to an increase in x_e where we take for simplicity $x_e = x_e^0 + \delta n_e/2$ and accordingly $x_h = x_e - \delta n_e$. Since our treatment with a constant Γ_0^h and without the possibility of an AFM ordering is not adapted for an undoped system, we consider here only a limited range $\delta n_e = 0.1 - 0.2$. The change in $\rho(T)$ in Fig. 4(a) is quite dramatic at $\delta n_e = 0.2$. This is a direct consequence of nearly vanishing $x_h \sim 0$ where the interband scattering becomes ineffective at low ω . Such a situation in real IPs corresponds to the well overdoped case. Clearly, our simplified analysis becomes insufficient beyond this point. Also $S(T)$ shows a similar trend, since at highest doping it becomes entirely FL-like with $S = \alpha T$ with a modest α .

Finally, let us turn to the comparison of our results with the experimental data on electron-doped IPs. Due to the phenomenological character of our theory as well as different IP material classes with quite different properties only a semi-quantitative comparison makes sense. Our central goal is to reproduce quite systematic variation of transport properties

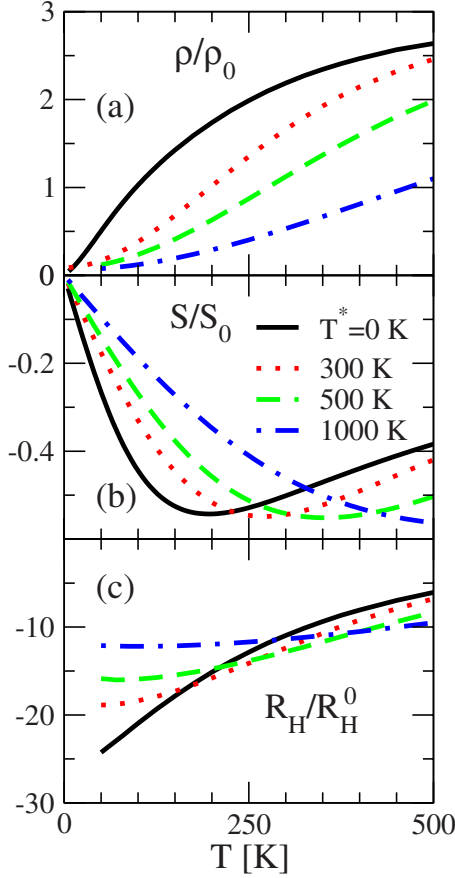


FIG. 3. (Color online) (a) Resistivity $\rho(T)/\rho_0$, (b) thermopower $S(T)/S_0$, and (c) the Hall constant $R_H(T)/R_H^0$ for different Fermi-liquid temperatures T^* and fixed concentrations $x_e=0.2$, $x_h=0.08$.

with doping, from low electron doping over the intermediate regime (optimal doping with highest T_c) to the overdoped one where SC disappears and IPs become rather normal FL-type metals. In our approach the doping dependence enters primarily through the electron/hole concentration difference δn_e . But as well, it is plausible that also the spin-fluctuation spectra $\tilde{\chi}''(\omega)$ change, being strong and anomalous at low doping, and on the other hand, at intermediate doping weaker and more FL-type in the low- ω regime. Within our analysis we can partly simulate the latter development with increasing T^* .

In the most challenging intermediate-doping regime our transport results match reasonably recent experiments on single crystals of the Co-doped BaFe_2As_2 compound. Note that BaFeCoAs with $x=0.1$ at $T=300$ K typically reveal $\rho \sim 0.3$ m Ω cm with a rather T -linear variation and corresponding slope $d\rho/dT \sim 0.5$ $\mu\Omega$ cm/K.^{16–18} As shown in Fig. 2(a) the value (note that $\tilde{\rho}_0=0.5$ m Ω cm) and the slope are reproduced within a factor of 3–4. While the magnitude of ρ is mostly governed by the spin-fermion coupling g_0 and can be fitted to experiments accordingly, it is essential that our analysis also reproduces the anomalous variation of $S(T)$. Recent data on BaFeCoAs at $x \sim 0.15$ reveal an abrupt increase in electronlike thermopower with a maximum value $|S| \sim 0.6s_0$ at $T=T_0 \sim 100$ K.¹⁸ For $T > T_0$ $|S|$ is decreasing in value. Both these features as well as values are well reproduced in Fig. 2(b).

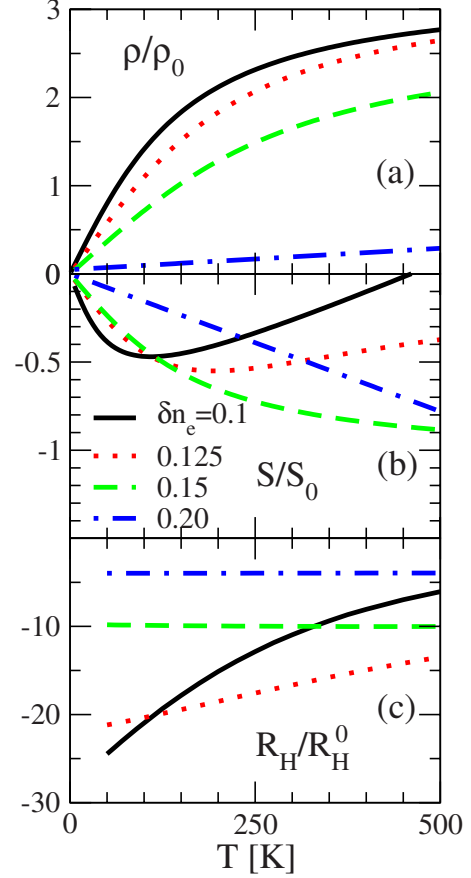


FIG. 4. (Color online) (a) Resistivity $\rho(T)/\rho_0$, (b) thermopower $S(T)/S_0$, and (c) the Hall constant $R_H(T)/R_H^0$ for $T^*=0$ and various electron doping δn_e with respect to the parent $x_e^0=x_h^0=0.15$ case.

With increasing Co doping in BaFeCoAs , $x > 0.1$, the resistivity behavior becomes closer to $\rho(T) \propto T^2$ not so much reduced in value at $T \sim 300$ K.^{16,17} In our analysis this corresponds to a change obtained by increasing the FL temperature $T^* > 0$ with a simultaneous increase in δn_e as presented in Figs. 3(a) and 4(a). Even more pronounced change in character is in $S(T)$ (Ref. 18) since it reduces in value, loses the minimum, and becomes FL-like, i.e., $S = \alpha T$. Such a development is well visible in Figs. 3(b) and 4(b) since both increasing $T^* > 0$ and δn_e lead to a crossover to a normal FL with a moderate slope α .

Experiments on the Hall constant reveal an electronlike $R_H < 0$ with a pronounced T dependence^{17,18} which reduces in the overdoped regime where at the same time it becomes consistent with the quasiclassical picture $R_H/R_H^0 \sim -1/x_e$. Our results in Figs. 3(c) and 4(c) show that both $T^* > 0$ as well as $\delta n_e > 0$ lead to a constant FL-like R_H . The particular value at $T \rightarrow 0$ from our analysis is less reliable. While at weak coupling we recover the expected $R_H/R_H^0 \sim -1/x_e$ (for $\rho_e \ll \rho_h$) the value can deviate for larger coupling since the approximations do not satisfy the Luttinger-volume sum rule. Note, however, that also the basic approximation Eq. (12) is not well understood yet.^{30,32}

Qualitatively similar results for transport quantities have been previously obtained for polycrystalline samples of the electron-doped LFAO family¹² discussed previously within

the same phenomenological framework.²¹ While our present data with assumed parameters would quite well match the measured $S(T)$,¹⁰ reported $\rho(T)$ as well as the slope $d\rho/dT$ (Ref. 12) are higher than in BaFeCoAs by a factor ~ 5 . It seems indicative that also recent single-crystal data¹⁵ do not reduce these values. From our present analysis this would require larger $g_0 \gg 1$ which could open the question of entering the (too) strong coupling regime.

VI. DISCUSSION

In conclusion, let us first put the present theoretical approach and its possible extensions in the perspective of related theoretical approaches, in particular those treating the QP, magnetic, and transport quantities in IPs. In contrast to many attempts to start with a more complete microscopic model,²² our approach is restricted to the simplest prototype two-band model coupled via spin fluctuations. These are taken as a phenomenological input of the marginal FL type whose deviation from the normal FL behavior is controlled by the crossover temperature T^* . Our analysis clearly indicates that the coupling appears not to be weak [at least as deduced from observed $\rho(T)$] and that spin fluctuations are quite strong in the low- ω regime as evidenced by INS experiments.⁵ It is therefore expected that our analysis can go beyond the weak-coupling approximation, being the basis, e.g., for a random-phase-approximation-type treatment of many-orbital models. The latter has been tested so far mostly on reproducing the proper band structure and on a qualitative description of relevant normal-state instabilities, in particular the most challenging SC onset. Evidently, our approach goes beyond the simple nesting scenario of the QP

damping as well as of the SC pairing since in the latter wave vector (\mathbf{k}, \mathbf{q}) dependences would play an essential role.

Interpreting our results for anomalous transport properties of IPs, we argue that they emerge as the interplay of several ingredients. First of all, observed $\rho(T)$ requires large interband coupling since the transport becomes quite normal and modest when the electron doping depletes the hole band, i.e., on approaching $x_h \sim 0$. The magnetic origin of the coupling is quite natural since it is intimately connected to the AFM (SDW) instability in the parent material and leads to an analogy with the physics of SC cuprates.

Highly nontrivial $S(T)$ in our analysis can be mostly related to two effects: (a) asymmetric variation of the QP damping $\Gamma^e(\omega)$ being the consequence of asymmetric DOS $\mathcal{N}^h(\omega)$ due to the closeness of the top of the hole band; and (b) small ϵ_e^0 which plays a role of the electron Fermi energy entering directly the expected FL behavior $S \sim \pi^2 T / 3 \epsilon_e^0$.

There are still several open questions even within the presented framework. Generally, stronger interband coupling leads to strong damping of minority QP which requires the treatment beyond the weak coupling. The same obstacle arises in the treatment of the parent and a weakly doped semimetal, where also experiments indicate very incoherent transport above $T > T_c$. Also, a comparison with experimental results for particular compounds could lead to refined models to reach a closer quantitative agreement.

ACKNOWLEDGMENTS

One of us (P.P.) acknowledges the fruitful discussion with T. Tohyama. This work was supported in part by the Slovenian Agency for Research and Development and by MHEST and JPSJ under the Slovenia-Japan Research Cooperative Program.

¹Y. Kamihara, T. Watanabe, M. Hirano, and H. Hosono, J. Am. Chem. Soc. **130**, 3296 (2008).

²For a review see H. Hosono and Z.-A. Ren, New J. Phys. **11**, 025003 (2009); K. Ishida, Y. Nakai, and H. Hosono, J. Phys. Soc. Jpn. **78**, 062001 (2009).

³M. Imada, A. Fujimori, and Y. Tokura, Rev. Mod. Phys. **70**, 1039 (1998).

⁴C. de la Cruz, Q. Huang, J. W. Lynn, Jiying Li, W. Ratcliff II, J. L. Zarestky, H. A. Mook, G. F. Chen, J. L. Luo, N. L. Wang, and Pengcheng Dai, Nature (London) **453**, 899 (2008).

⁵D. S. Inosov, J. Park, P. Bourges, D. Sun, Y. Sidis, A. Schneidewind, K. Hradil, D. Haug, C. Lin, B. Keimer, and V. Hinkov, Nature Physics **6**, 178 (2009).

⁶M. D. Lumsden, A. D. Christianson, D. Parshall, M. B. Stone, S. E. Nagler, G. J. MacDougall, H. A. Mook, K. Lokshin, T. Egami, D. L. Abernathy, E. A. Goremychkin, R. Osborn, M. A. McGuire, A. S. Sefat, R. Jin, B. C. Sales, and D. Mandrus, Phys. Rev. Lett. **102**, 107005 (2009).

⁷S. Chi, A. Schneidewind, J. Zhao, L. W. Harriger, L. Li, Y. Luo, G. Cao, Z. Xu, M. Loewenhaupt, J. Hu, and P. Dai, Phys. Rev. Lett. **102**, 107006 (2009).

⁸H. Mukuda, N. Terasaki, N. Tamura, H. Kinouchi, M. Yashima, Y. Kitaoka, K. Miyazawa, P. M. Shirage, S. Suzuki, S. Mi-

yasaka, S. Tajima, H. Kito, H. Eisaki, and A. Iyo, J. Phys. Soc. Jpn. **78**, 084717 (2009).

⁹F. L. Ning, K. Ahilan, T. Imai, A. S. Sefat, M. A. McGuire, B. C. Sales, D. Mandrus, P. Cheng, B. Shen, and H. -H. Wen, Phys. Rev. Lett. **104**, 037001 (2010).

¹⁰A. S. Sefat, M. A. McGuire, B. C. Sales, R. Jin, J. Y. Howe, and D. Mandrus, Phys. Rev. B **77**, 174503 (2008).

¹¹S. C. Lee, A. Kawabata, T. Moyoshi, Y. Kobayashi, and M. Sato, J. Phys. Soc. Jpn. **78**, 043703 (2009).

¹²C. Hess, A. Kondrat, A. Narduzzo, J. E. Hamann-Borrero, R. Klingeler, J. Werner, G. Behr, and B. Büchner, Europhys. Lett. **87**, 17005 (2009).

¹³H. Eisaki, A. Iyo, H. Kito, K. Miyazawa, P. M. Shirage, H. Matsuhata, K. Kihou, C. H. Lee, N. Takeshita, R. Kumai, Y. Tomioka, and T. Ito, J. Phys. Soc. Jpn. **77**, Suppl. C, 36 (2008); K. Miyazawa, K. Kihou, P. M. Shirage, C.-H. Lee, H. Kito, H. Eisaki, and A. Iyo, *ibid.* **78**, 034712 (2009).

¹⁴Y. Ando, A. N. Lavrov, S. Komiyama, K. Segawa, and X. F. Sun, Phys. Rev. Lett. **87**, 017001 (2001); Y. Ando, S. Komiyama, K. Segawa, S. Ono, and Y. Kurita, *ibid.* **93**, 267001 (2004).

¹⁵A. Jesche, C. Krellner, M. de Souza, M. Lang, and C. Geibel, New J. Phys. **11**, 103050 (2009).

¹⁶L. Fang *et al.*, Phys. Rev. B **80**, 140508(R) (2009).

- ¹⁷F. Rullier-Albenque, D. Colson, A. Forget, and H. Alloul, Phys. Rev. Lett. **103**, 057001 (2009).
- ¹⁸E. D. Mun, S. L. Budko, N. Ni, A. N. Thaler, and P. C. Canfield, Phys. Rev. B **80**, 054517 (2009).
- ¹⁹J. R. Cooper and J. W. Loram, J. Phys. (France) **6**, 2237 (1996).
- ²⁰Y. Kohama, Y. Kamihara, S. Riggs, F. F. Balakirev, T. Atake, M. Jaime, M. Hirano, and H. Hosono, Europhys. Lett. **84**, 37005 (2008).
- ²¹P. Prelovšek, I. Sega, and T. Tohyama, Phys. Rev. B **80**, 014517 (2009).
- ²²For a theoretical overview, see I. I. Mazin and J. Schmalian, arXiv:0901.4790 (unpublished).
- ²³S. Raghu, X.-L. Qi, C.-X. Liu, D. J. Scalapino, and S.-C. Zhang, Phys. Rev. B **77**, 220503(R) (2008).
- ²⁴W.-Q. Chen, K.-Y. Yang, Y. Zhou, and F.-C. Zhang, Phys. Rev. Lett. **102**, 047006 (2009).
- ²⁵M. M. Korshunov and I. Eremin, Europhys. Lett. **83**, 67003 (2008).
- ²⁶A. V. Chubukov, arXiv:0902.4188 (unpublished).
- ²⁷C. M. Varma, P. B. Littlewood, S. Schmitt-Rink, E. Abrahams, and A. E. Ruckenstein, Phys. Rev. Lett. **63**, 1996 (1989).
- ²⁸G. D. Mahan, *Many-Particle Physics* (Kluwer Academic, Dordrecht, 2000).
- ²⁹G. Palsson and G. Kotliar, Phys. Rev. Lett. **80**, 4775 (1998).
- ³⁰P. Voruganti, A. Golubentsev, and S. John, Phys. Rev. B **45**, 13945 (1992).
- ³¹H. Kohno and Y. Yamada, Prog. Theor. Phys. **80**, 623 (1988).
- ³²K. Haule, A. Rosch, J. Kroha, and P. Wölfle, Phys. Rev. B **68**, 155119 (2003).
- ³³J. Merino and R. H. McKenzie, Phys. Rev. B **61**, 7996 (2000).
- ³⁴See the review by K. Kontani, Rep. Prog. Phys. **71**, 026501 (2008).